Translational Oncology
www.transonc.com

Volume 6 Number 2 April 2013 pp. 206–215 206

FAK Inhibition Decreases Hepatoblastoma Survival Both *In Vitro* and *In Vivo*[1,2]

Lauren A. Gillory*, Jerry E. Stewart*, Michael L. Megison*, Hugh C. Nabers*, Elizabeth Mroczek-Musulman† and Elizabeth A. Beierle*

*Department of Surgery, University of Alabama at Birmingham, Birmingham, AL; †Department of Pathology, Children's of Alabama, Birmingham, AL

Abstract

Hepatoblastoma is the most frequently diagnosed liver tumor of childhood, and children with advanced, metastatic or relapsed disease have a disease-free survival rate under 50%. Focal adhesion kinase (FAK) is a nonreceptor tyrosine kinase that is important in many facets of tumor development and progression. FAK has been found in other pediatric solid tumors and in adult hepatocellular carcinoma, leading us to hypothesize that FAK would be present in hepatoblastoma and would impact its cellular survival. In the current study, we showed that FAK was present and phosphorylated in human hepatoblastoma tumor specimens. We also examined the effects of FAK inhibition upon hepatoblastoma cells using a number of parallel approaches to block FAK including RNAi and small molecule FAK inhibitors. FAK inhibition resulted in decreased cellular survival, invasion, and migration and increased apoptosis. Further, small molecule inhibition of FAK led to decreased tumor growth in a nude mouse xenograft model of hepatoblastoma. The findings from this study will help to further our understanding of the regulation of hepatoblastoma tumorigenesis and may provide desperately needed novel therapeutic strategies and targets for aggressive, recurrent, or metastatic hepatoblastomas.

Translational Oncology (2013) 6, 206–215

Introduction

Hepatoblastoma is the most frequently diagnosed malignant liver tumor in children. These tumors originate from immature liver precursor cells and likely result from a developmental disturbance causing aberrant cellular proliferation [1]. Although chemotherapy in conjunction with radical surgical resection has improved the prognosis for patients with hepatoblastoma [2], disease-free survival rates remain less than 50% for patients with advanced, metastatic or relapsed disease. For this reason, novel therapeutic options are needed for the treatment of these children.

Focal adhesion kinase (FAK) is a nonreceptor protein tyrosine kinase that has been found to regulate cellular signaling pathways for multiple functions, such as adhesion, proliferation, and survival. Integrins bind to the β subunits of FAK, leading to FAK phosphorylation and the binding of Src family kinases, resulting in a FAK-Src complex, which promotes cellular migration and growth [3]. FAK is also activated by autophosphorylation at the tyrosine 397 (Y397) residue, which results in downstream survival signaling through activation of phosphatidylinositol 3′-kinase (PI3K) and increased expression of inhibitor of apoptosis proteins [4]. FAK has been shown to be overexpressed and to correlate with tumor aggressiveness in a number of human tumors including breast and colon cancer [5] and the pediatric solid tumor neuroblastoma [6]. Abrogation of FAK with multiple modalities including small interfering RNA (siRNA) [7], AdFAK-CD [8,9], and small molecule inhibitors [10–12] has been shown to decrease cellular migration and survival in multiple tumor types.

Investigators have found FAK expression in hepatocellular carcinoma tumor specimens and cell lines, and FAK augmented the invasive and metastatic potential in these tumors [13]. Knowing the importance of FAK in other tumor types and with the data from the hepatocellular

Address all correspondence to: Elizabeth A. Beierle, MD, 1600 7th Avenue South, Lowder Building, Room 300, Birmingham, AL 35233.
E-mail: elizabeth.beierle@childrensal.org

[1]This work was supported by grants from the National Cancer Institute [T32CA091078 to L.A.G. and M.L.M. and K08CA118178 to E.A.B.]. The content of this manuscript was solely the responsibility of the authors and does not necessarily represent the official views of the National Cancer Institute. Conflict of Interest Statement: None declared.
[2]This article refers to supplementary material, which is designated by Figure W1 and is available online at www.transonc.com.
Received 27 December 2012; Revised 29 January 2013; Accepted 29 January 2013

1944-7124/13 DOI 10.1593/tlo.12505

carcinoma studies, we hypothesized that FAK would be present in hepatoblastoma and would impact cellular survival in this liver tumor. To confirm our hypotheses, we used immunohistochemistry to illustrate the presence of FAK in human hepatoblastoma specimens and immunoblot analysis to determine FAK expression in the HuH6 hepatoblastoma cell line. Furthermore, we illustrated that FAK inhibition with siRNA and small molecule inhibitors resulted in decreased cellular invasion and viability *in vitro* and decreased hepatoblastoma xenograft growth *in vivo*. These studies demonstrated that targeting FAK may present a novel treatment strategy for hepatoblastoma.

Materials and Methods

Tumor Specimens and Cell Line

Formalin-fixed, paraffin-embedded hepatoblastoma specimens were obtained from our institution after Institutional Review Board approval (X111123007). The Institutional Review Board waived the need for informed consent since the specimens were previously obtained for the purposes of diagnosis and treatment. The hepatoblastoma cell line, HuH6, was kindly provided by Dr Thomas Pietschmann [14]. The HuH6 cell line was maintained at 37°C and 5% CO_2 in Dulbecco's modified Eagle's medium with 10% FBS, 2 mM L-glutamine, and 1 μg/ml penicillin/streptomycin. The mouse endothelial fibroblasts with ($MEF^{FAK+/+}$) and without ($MEF^{FAK-/-}$) FAK expression were a kind gift from Dr Elena Kurenova. These cell lines were maintained in Dulbecco's modified Eagle's medium with 10% FBS, 2 mM L-glutamine, and 1 μg/ml penicillin/streptomycin at 37°C and 5% CO_2.

Antibodies and Reagents

Antibodies used for Western blot analysis were given as follows: Mouse monoclonal anti-FAK (4.47) and rabbit polyclonal anti–phospho-FAK (Y397) antibodies were obtained from EMD Millipore (Billerica, MA; 05-537) and Invitrogen Corp (Carlsbad, CA; 4624G), respectively. Antibody for cleaved poly (ADP-ribose) polymerase (PARP) was from Cell Signaling Technology, Inc (Danvers, MA; 9542s, rabbit polyclonal). Glyceraldehyde 3-phosphate dehydrogenase (GAPDH) antibody was from Fitzgerald Industries International (Acton, MA; 10R-1178) and β-actin antibody was from Santa Cruz Biotechnology, Inc (Santa Cruz, CA).

siRNA was obtained from Qiagen Inc (Valencia, CA) and used as previously described [15]. Briefly, cells were plated and allowed to attach for 24 hours and were then transfected with Hyperfect (Qiagen Inc) alone, Hyperfect (Qiagen Inc) plus control siRNA (AllStars Negative Control siRNA; Qiagen Inc), or Hyperfect (Qiagen Inc) plus FAK siRNA [Hs_PTK2_10 FlexiTube siRNA (NM_005607, NM_153831); Qiagen Inc] according to the manufacturer's protocol. Cells were incubated for 24 to 72 hours after transfection and then used for experiments.

The small molecules PF-573,228 (PF) and 1,2,4,5-benzenetetraamine tetrahydrochloride ($C_6H_{10}N_4{\cdot}4ClH$; Y15) were obtained from Santa Cruz Biotechnology, Inc.

Immunohistochemistry

Formalin-fixed, paraffin-embedded tumor blocks for the human specimens or murine xenografts were cut in 8-μm sections. The slides were baked for 1 hour at 70°C, deparaffinized, rehydrated, and steamed. The sections were then quenched with 3% hydrogen peroxide and blocked with phosphate-buffered saline–blocking buffer. The primary antibodies, anti-FAK 4.47 (1:100, mouse monoclonal, 05-537; EMD Millipore) and anti–phospho-FAK (Y397) (1:200, rabbit polyclonal, 4624G; Invitrogen Corp), were added and incubated overnight at 4°C. After washing with phosphate-buffered saline, the secondary antibodies were added at 1:250 dilution (Jackson ImmunoResearch Laboratories, Inc, West Grove, PA) for 1 hour at 22°C. The staining reaction was developed with VECTASTAIN Elite ABC Kit (PK-6100; Vector Laboratories, Burlingame, CA), TSA (Biotin Tyramide Reagent, 1:400; PerkinElmer, Inc, Waltham, MA), and DAB (Metal Enhanced DAB Substrate; Thermo Fisher Scientific, Rockford, IL). Slides were counterstained with hematoxylin. Negative controls [mouse IgG (1 μg/ml; Invitrogen Corp) or rabbit IgG (1 μg/ml; EMD Millipore)] were included with each run.

Immunohistochemistry Scoring

A single board-certified pathologist (E.M.M.), blinded to the specimens, reviewed each human tissue section for FAK and phosphor-FAK and assigned a stain score. Scoring was based on a system that has been used previously [6]. The slides were examined and the staining evaluated by measuring the intensity of stain (0, none; 1, weak; 2, moderate; 3, strong; 4, extremely strong) and the percentage of positive cells (0–100). A stain score was calculated based on the percent positive cells and the amount of staining. For instance, if the specimen showed moderate staining (2) in 70% of the cells, the calculated stain score would be $2 \times 70 = 140$.

Immunoblot Analysis

Western blots were performed as previously described [12]. Briefly, cells or homogenized xenograft specimens were lysed on ice for 30 minutes in a buffer containing 50 mM Tris-HCl (pH 7.5), 150 mM NaCl, 1% Triton X-100, 0.5% NaDOC, 0.1% sodium dodecyl sulfate (SDS), 5 mM EDTA, 50 mM NaF, 1 mM $NaVO_3$, 10% glycerol, and protease inhibitors: 10 μg/ml leupeptin, 10 μg/ml phenylmethylsulfonyl fluoride (PMSF), and 1 μg/ml aprotinin. The lysates were cleared by centrifugation at 10,000 rpm for 30 minutes at 4°C. Protein concentrations were determined using a Bio-Rad kit (Bio-Rad, Hercules, CA) and proteins were separated by electrophoresis on SDS–polyacrylamide gel electrophoresis gels. Antibodies were used according to the manufacturer's recommended conditions. Molecular weight markers (Precision Plus Protein Kaleidoscope Standards; Bio-Rad) were used to confirm the expected size of the target proteins. Immunoblots were developed with chemiluminescence (Amersham ECL Western Blotting Detection Reagents; GE Healthcare Life Sciences, Piscataway, NJ). Blots were stripped with stripping solution (Bio-Rad) at 37°C for 15 minutes and then reprobed with selected antibodies. Immunoblot analysis with antibody to β-actin or GAPDH provided an internal control for equal protein loading.

Cell Viability Assays

Equal numbers of cells were plated and allowed to attach for 24 hours. Cells were treated with RNAi inhibition, PF, or Y15, and cell viability was measured using alamarBlue assay. In brief, 1.5×10^3 cells per well were plated onto 96-well culture plates and allowed to attach. Following treatment, 10 μl of alamarBlue dye was added to 200 μl of cell medium. After 4 to 6 hours, the absorbance at 595 nm was measured using a kinetic microplate reader (BioTek Gen5; BioTek Instruments, Winooski, VT). Cell viability was also studied using trypan blue exclusion and cell counting with a hemacytometer. Viability was reported as fold change.

Cellular Invasion Assay

Twelve-well culture plates with 8-μm micropore inserts were used for cell invasion assays. The top side of the insert was coated with Matrigel (BD Biosciences, San Jose, CA; 1 mg/ml, 50 μl for 4 hours at 37°C). Cells were treated with PF or Y15 and 3×10^5 cells were placed into the upper well, cultured for 48 hours and allowed to invade into the Matrigel layer. The cells on the inserts were fixed with 3% paraformaldehyde, stained with crystal violet, and counted with a light microscope. Invasion was reported as fold change in number of cells invading into the Matrigel.

Migration Assay

Similar to invasion, 12-well culture plates with 8-μm micropore inserts were used for cell migration assays, with the bottom side of the insert coated with collagen (MP Biomedicals, Thermo Fisher Scientific; 1 mg/ml, 50 μl for 4 hours at 37°C). Cells were treated with PF or Y15 and 3×10^5 cells were placed into the upper well, cultured for 24 hours, and allowed to invade through the transwell plate. The cells on the inserts were fixed with 3% paraformaldehyde, stained with crystal violet, and counted with a light microscope. Migration was reported as fold change in number of cells migrating through the transwell plate.

Attachment-Independent Growth Assay

Attachment-independent growth was determined by soft agar assay. A base layer of complete culture media in 1% noble agar was established in 60-mm culture dishes. HuH6 cells were plated at 1×10^4 cells per dish in the top layer composed of the same culture media and agar mixture. Dishes were treated with graduated concentrations of PF or Y15. After incubation for 12 days, colonies were imaged and quantified using the Gel Dock Imager (Bio-Rad) and Quantity One Software (Bio-Rad), respectively. Colony counts were reported as means ± SEM.

Apoptosis Assays

Apoptosis was detected by measuring activation of caspase-3 (Caspase-3/CPP32 Colorimetric Protease Assay; Invitrogen Corp) according to the manufacturer's instructions. Briefly, cells were treated with PF or Y15 and plated onto 96-well plates. After 48 hours, cells were lifted and lysed. Cell lysates were incubated in reaction buffer containing DTT and DEVD-pNA substrate and read at 405 nm using a kinetic microplate reader (BioTek Gen5). Caspase-3 activation was reported as fold change in activation. Apoptosis was also documented by immunoblot analysis for PARP cleavage. Cells were treated with PF or Y15; lysates were collected, and immunoblot analysis for cleaved PARP was performed. Bands were detected by chemiluminescence and β-actin served as an internal control.

Tumor Growth In Vivo

Six-week-old, female, athymic nude mice were used (Harlan Laboratories, Inc, Chicago, IL). The mice were maintained in an specific pathogen free (SPF) animal facility with standard 12-hour light/dark cycles and allowed chow and water *ad libitum*. All experiments were performed after obtaining protocol approval from the Animal Care and Use Committee (110209355) and in compliance with the institutional, national, and National Institutes of Health animal use guidelines. Human hepatoblastoma cells, HuH6 (2×10^6 cells) in Matrigel (BD Biosciences), were injected subcutaneously into the right flank.

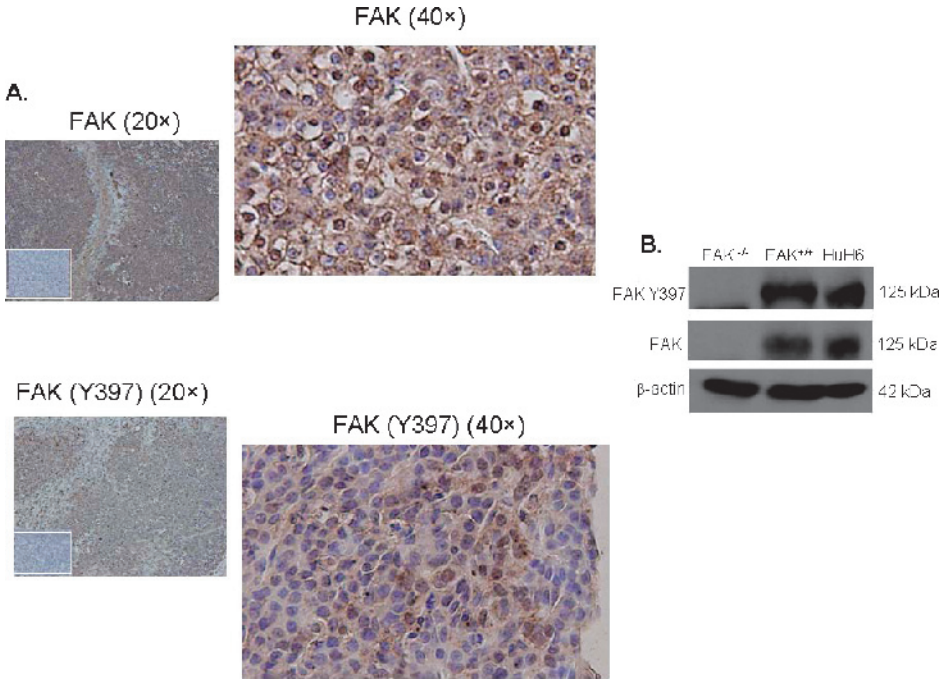

Figure 1. FAK in hepatoblastoma human specimens and HuH6 cell line. Immunohistochemistry staining with antibodies specific for FAK and phospho-FAK was performed on 28 formalin-fixed, paraffin-embedded human hepatoblastoma specimens. (A) Representative photomicrographs show staining of the hepatoblastoma cells for FAK and phospho-FAK. Negative controls (lower white inserts, left panels) were included with each run. FAK staining was detected in 23 of 28 specimens (top panels) and was phosphorylated in 71% (bottom panels). (B) Immunoblot analysis for Y397 FAK and total FAK was performed on HuH6 hepatoblastoma cell lysates. There was FAK present and it was phosphorylated at the Y397 site. Lysates from mouse endothelial fibroblasts with ($MEF^{FAK+/+}$) and without ($MEF^{FAK-/-}$) FAK served as positive and negative controls, respectively.

Animals were treated twice daily with intraperitoneal injections of control vehicle (normal saline, $N = 9$) or Y15 (30 mg/kg/day, $N = 10$). Previous experiments with various doses and dosing schedules of the compound proved this dosage to be well tolerated [10–12]. Tumors were measured twice weekly with a caliper and tumor volume in mm^3 was calculated using the standard formula [(width)^2 × length]/2, where width was the smaller diameter. When control tumors reached the volume allowed by the Institutional Animal Care and Use Committee (IACUC) protocol (after 3 weeks of treatment), the animals were killed with CO_2 and bilateral thoracotomy, and the tumors were harvested.

Data Analysis

Experiments were repeated at least in triplicate, and data are reported as means ± SEM. An analysis of variance or Student's *t* test was used as appropriate to compare data between groups. Statistical significance was determined at the $P < .05$ level.

Results

FAK Was Present in Hepatoblastoma Human Specimens and Cell Line

Immunohistochemistry was performed on 28 human hepatoblastoma specimens. FAK staining was detected in 23 of 28 specimens and was phosphorylated in 19 of the 28 specimens (71%; Figure 1*A*). The stain scores for FAK ranged from 0 to 140, with a mean FAK stain score of 33.7 ± 8.1. Immunoblot analysis revealed that the HuH6 cell line expressed FAK and that FAK was phosphorylated at the Y397 site (Figure 1*B*). Mouse endothelial fibroblasts with ($MEF^{FAK+/+}$) and without ($MEF^{FAK-/-}$) FAK were used for comparison (Figure 1*B*).

FAK Inhibition with RNA Silencing Led to Decreased Hepatoblastoma Viability

Since FAK regulates cell survival, we investigated the effects of FAK silencing with siRNA on hepatoblastoma viability. Treatment with FAK siRNA (20 and 40 nM) for 24 hours successfully inhibited FAK protein expression in HuH6 cells (Figure 2*A*). HuH6 cell viability was measured with trypan blue after abrogation of FAK with siRNA for 24 hours. Cell death increased significantly after treatment with FAK siRNA at 20 nM (Figure 2*B*) and more than two-fold after treatment with 40 nM FAK siRNA compared to control (Figure 2*B*). Control siRNA did not alter FAK expression (Figure 2*A*) or significantly increase HuH6 cell death (Figure 2*B*). We concluded that silencing FAK with siRNA significantly decreased viability in HuH6 cells.

PF Inhibited Phosphorylation of FAK in Human Hepatoblastoma Cells and Led to Decreased Viability, Invasion, and Migration and Increased Apoptosis

We wished to further examine the effects of FAK inhibition using a small molecule FAK inhibitor. PF has been shown to decrease FAK phosphorylation [17]. HuH6 cells were treated with increasing concentrations of PF for 48 hours, and immunoblot analysis was used to detect FAK expression and phosphorylation. PF treatment of the HuH6 cells led to decreased phosphorylation of FAK Y397 (Figure 3*A*). Next, we wished to determine if PF-induced loss of FAK phosphorylation resulted in decreased cell survival. AlamarBlue assays were used to evaluate cell viability after treatment with PF. After 48 hours of PF treatment, there was a statistically significant decrease in viability (Figure 3*B*). At a PF concentration of 5 μM, cell viability decreased to 25 ± 3.0%

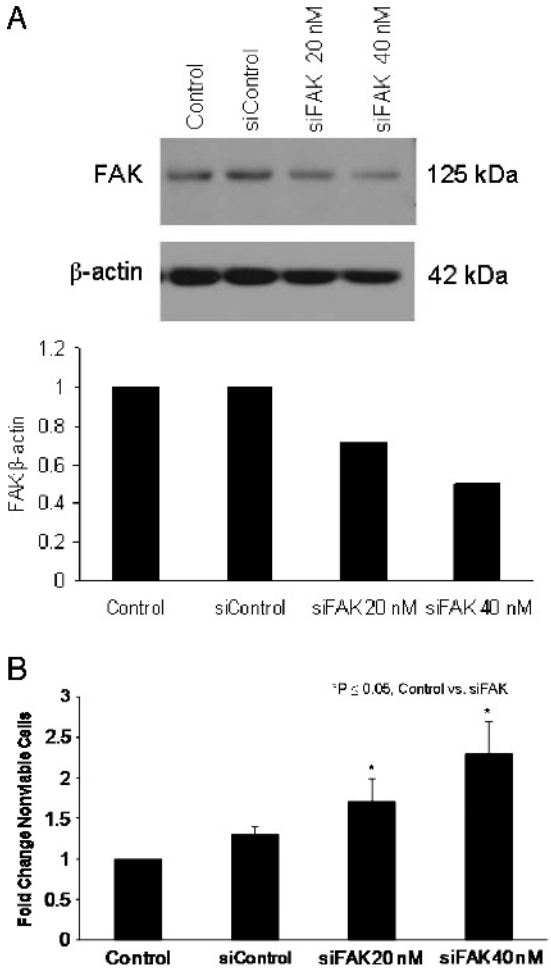

Figure 2. FAK inhibition with siRNA in HuH6 human hepatoblastoma cells. (A) The HuH6 cells were treated with FAK siRNA or control siRNA. Immunoblot analysis was used to confirm FAK protein knockdown. After treatment with FAK siRNA for 24 hours, there was a decrease in FAK protein expression. Densitometry was used to quantitate FAK inhibition, with FAK expressed relative to the β-actin bands (*bottom graph*). (B) HuH6 cells were treated with FAK siRNA at 20 and 40 nM for 24 hours and cell viability was measured using trypan blue assay. There was a significant increase in the number of nonviable cells after siRNA treatment. The control siRNA had no effect on cellular viability.

compared to control ($P \leq .01$; Figure 3*B*). The calculated lethal concentration 50 for PF in the HuH6 cells was 4 μM.

In addition to being important in cell survival, FAK also plays a role in cellular invasion and migration [16]. Since PF treatment resulted in a loss of FAK phosphorylation, we decided to investigate the effects of PF on HuH6 invasion and migration. Cells were treated with PF for 48 hours and transwell invasion assays were used. Treatment with PF decreased cellular invasion to 72 ± 10.0% of control at 2.5 μM concentration (Figure 3*C*). For migration, cells were treated with PF and their ability to migrate through a transwell plate was measured. Treatment with PF resulted in a decrease in cellular migration that reached significance at 2.5 μM concentration (Figure 3*D*). Finally, the impact of FAK inhibition on attachment-independent growth through the formation of colonies in soft agar was studied. HuH6 cells were treated with PF, grown in soft agar for 12 days, and colonies were quantified. Colony count was significantly decreased with PF treatment

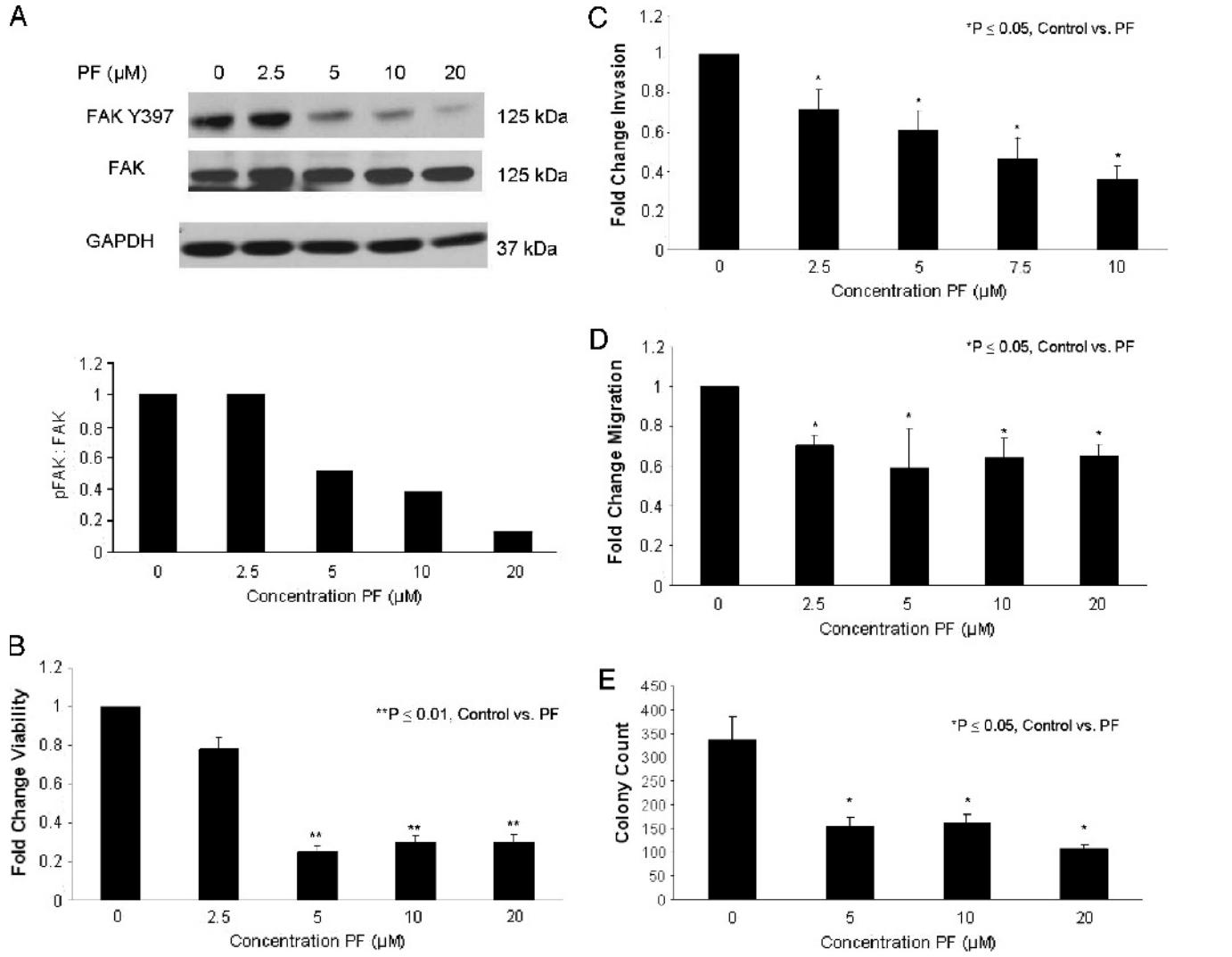

Figure 3. PF inhibition of FAK phosphorylation in human hepatoblastoma cells. (A) The HuH6 hepatoblastoma cell line was treated for 48 hours with increasing concentrations of PF and cell lysates were harvested. Immunoblot analysis was used to examine FAK Y397 phosphorylation and total FAK in the lysates. Densitometry was performed, and FAK phosphorylation was reported as a ratio between the density of the Y397 phospho-FAK band to the density of the total FAK band. Increasing concentrations of PF resulted in decreased FAK phosphorylation. (B) AlamarBlue assay was used to measure cell viability. HuH6 hepatoblastoma cells were treated with PF at increasing concentrations for 48 hours. Cellular viability was decreased with a PF concentration of 2.5 μM but did not reach statistical significance until the 5 μM concentration. (C) HuH6 cells were treated with increasing concentrations of PF and allowed to invade through a Matrigel-coated micropore insert. Invasion was reported as fold change. Cellular invasion was significantly decreased with PF beginning at the 2.5 μM concentration. (D) HuH6 cells were treated with increasing concentrations of PF and allowed to migrate through a micropore insert. Migration was reported as fold change in number of cells migrating through the membrane. Cellular migration was significantly decreased with PF treatment, and as seen with invasion, the effects of PF upon migration were significant at a concentration of 2.5 μM. (E) Attachment-independent growth in soft agar was used to further characterize tumor invasiveness. HuH6 cells were treated with increasing concentrations of PF, grown in soft agar for 12 days, and colonies were quantified. Colony count was significantly decreased with PF treatment compared to untreated cells.

compared to untreated cells (Figure 3*E*). These experiments illustrated that inhibition of FAK phosphorylation in HuH6 hepatoblastoma cells results in diminished cell viability, invasion, migration and attachment-independent growth.

Finally, since PF resulted in decreased cell survival, we examined the effects of PF on apoptosis in the HuH6 hepatoblastoma cell line. Apoptosis was measured with both a caspase activation kit and immunoblot analysis for PARP cleavage products. Caspase-3 was significantly activated after treatment with 10 μM PF for 48 hours (Figure 4*A*). To further document that the cells were undergoing apoptosis, HuH6 cells were treated with PF and lysates were examined with immunoblot analysis for PARP cleavage products. Treatment with PF led to an increase in cleaved PARP (Figure 4*B*), indicating that apoptosis was occurring in the HuH6 cells.

Y15 Inhibited FAK Phosphorylation in Human Hepatoblastoma Cells and Resulted in Decreased Cell Survival, Invasion, Migration, and Increased Apoptosis

We wished to move forward with animal studies, but PF was not formulated for *in vivo* studies [17]. Therefore, we chose to use Y15,

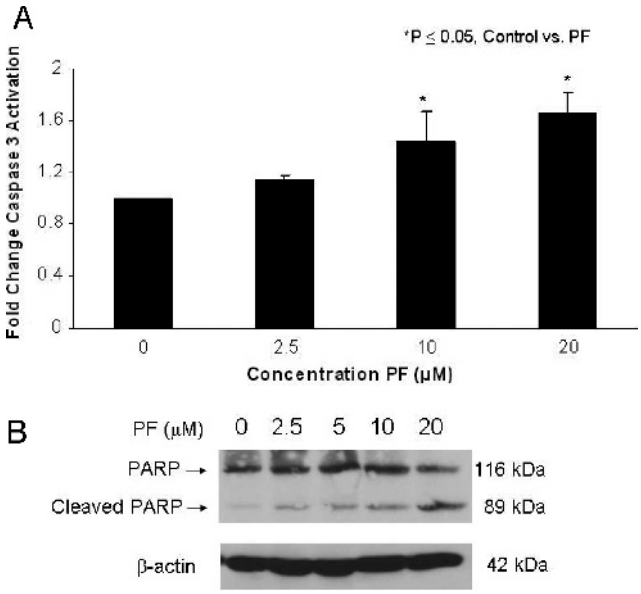

Figure 4. PF treatment of HuH6 cells resulted in cellular apoptosis. Since PF resulted in decreased cell survival, we examined the effects of PF on apoptosis in the HuH6 hepatoblastoma cell line. (A) HuH6 cells were treated for 48 hours with increasing concentrations of PF. Apoptosis was measured with a caspase activation kit. Caspase-3 was significantly activated after treatment with PF. (B) To further document that the cells were undergoing apoptosis, HuH6 cells were treated with PF at increasing concentrations for 48 hours, and lysates were examined with immunoblot analysis for PARP cleavage products. Treatment with PF led to an increase in cleaved PARP, again, indicating that PF led to apoptosis in the HuH6 cell line.

one of only a few small molecule FAK inhibitors that may be used in animals [10–12]. Y15 has been previously described and was designed to inhibit Y397 phosphorylation of FAK [10]. We established with immunoblot analysis that treatment with Y15 led to a decline in FAK phosphorylation in the HuH6 hepatoblastoma cells (Figure 5*A*). We next investigated whether this loss of Y397 FAK phosphorylation by Y15 would affect cell survival. Viability was detected with alamarBlue assay. Treatment with Y15 resulted in a decrease in hepatoblastoma cellular viability that was significant at a concentration of 5 μM (100 *vs* 56.1 ± 3.0%, control *vs* Y15; $P \leq 0.01$; Figure 5*B*).

Similar to the PF studies, we used transwell invasion and migration assays and growth in soft agar to further characterize the effects of Y15 on the HuH6 cell line. At a concentration of 2.5 μM, there was a statistically significant difference in cellular invasion and migration following Y15 treatment (Figure W1, *A* and *B*). Examining attachment-independent growth in soft agar, Y15 treatment (2.5 μM) decreased colony formation from 336 ± 52 to 137 ± 15 (control *vs* Y15, $P \leq 0.05$; Figure 5*C*). To determine whether Y15 caused apoptosis in the HuH6 hepatoblastoma cells, we used immunoblot analysis for PARP cleavage products and a caspase-3 activation assay. After a 48-hour treatment with Y15, there was an increase in PARP cleavage products with increasing Y15 concentrations (Figure 5*D*). Furthermore, after treatment with 5 μM Y15, there was a statistically significant increase in activated caspase-3 (Figure 5*E*). Since these findings were similar to those seen with PF, we proceeded with animal studies using Y15 for FAK inhibition.

Treatment with Y15 Inhibited Growth of Human Hepatoblastoma Xenografts

To determine the *in vivo* effect of FAK inhibition upon hepatoblastoma, we used a nude mouse xenograft model. Human hepatoblastoma cells, HuH6, were injected subcutaneously into the right flank and mice were randomized at the time of injection to receive either saline (vehicle) control ($N = 9$) or Y15 ($N = 10$) beginning the day after cells were injected. Animals were treated twice daily with intraperitoneal injections of 15 mg/kg Y15. Treatment was discontinued and animals were killed at four weeks, the time point that the control tumors reached maximal size allowed by protocol. The Y15-treated animals did not demonstrate any obvious toxicity compared to controls. Treatment with Y15 resulted in a significant decrease in HuH6 tumor volume compared to vehicle-treated animals (Figure 6*A*).

Previous studies showed that Y15 did target FAK phosphorylation in tumor xenografts [10–12]. Therefore, we wished to determine whether Y15 treatment resulted in decreased phosphorylation of FAK *in vivo* for the HuH6 tumor xenografts. Tumor specimens were homogenized and lysates were collected. The tumor protein lysates were analyzed with immunoblot analysis for FAK (Y397) and total FAK. A representative immunoblot showing a decrease in FAK phosphorylation in those tumors treated with Y15 compared to those treated with vehicle was presented in Figure 6*B*. Densitometry of the blot showed a decrease in the phosphorylated FAK to total FAK ratio (Figure 6*B*, *top right graph*). Using densitometry evaluation of immunoblots from all of the *in vivo* tumor lysates, we determined that Y15 treatment decreased the pFAK/FAK ratio (Figure 6*B*, *bottom panel*) from 0.86 ± 0.10 to 0.36 ± 0.16 (control *vs* Y15, $P = .03$) in the protein lysates from the tumor xenografts. Representative photomicrographs at 20× of immunohistochemical staining for total and phosphorylated FAK of the formalin-fixed, paraffin-embedded xenograft samples were presented in Figure 6*C*. The larger images correspond to black boxes in photomicrographs. Immunohistochemical staining showed findings similar to immunoblot analysis; the tumors from the animals treated with Y15 had decreased FAK Y397 phosphorylation compared to the vehicle-treated tumors (*bottom row*). Negative controls were included in each immunohistochemical run (Figure 6*C*, *white inserts*).

Discussion

Hepatoblastoma continues to present a therapeutic challenge, and prognosis remains dismal for patients with advanced and metastatic disease, highlighting the need for novel treatments. In the current study, we investigated the role of FAK in hepatoblastoma tumorigenesis. Our rationale for studying FAK in hepatoblastoma was threefold. First, FAK has been shown to be important in another pediatric solid tumor, neuroblastoma. In neuroblastoma, FAK has been shown to regulate cell survival, adhesion, and invasive potential [6,15]. Second, FAK expression and phosphorylation have been found in the adult liver tumor, hepatocellular carcinoma. Chen et al. demonstrated that FAK expression correlated with tumor stage and vascular invasion in hepatocellular carcinoma [13]. In addition, other investigators have shown that in human hepatocellullar carcinoma tumor specimens, increased FAK mRNA abundance [18] and increased FAK protein expression [19] was associated with worse disease-free and overall survival. Finally, there have been other data in hepatoblastoma that indirectly indicated that FAK may be important in the tumorigenicity of this tumor. Hsiao recently showed that eight of eight hepatoblastoma tumor specimens overexpress Toll-like receptor 4 (TLR4) by

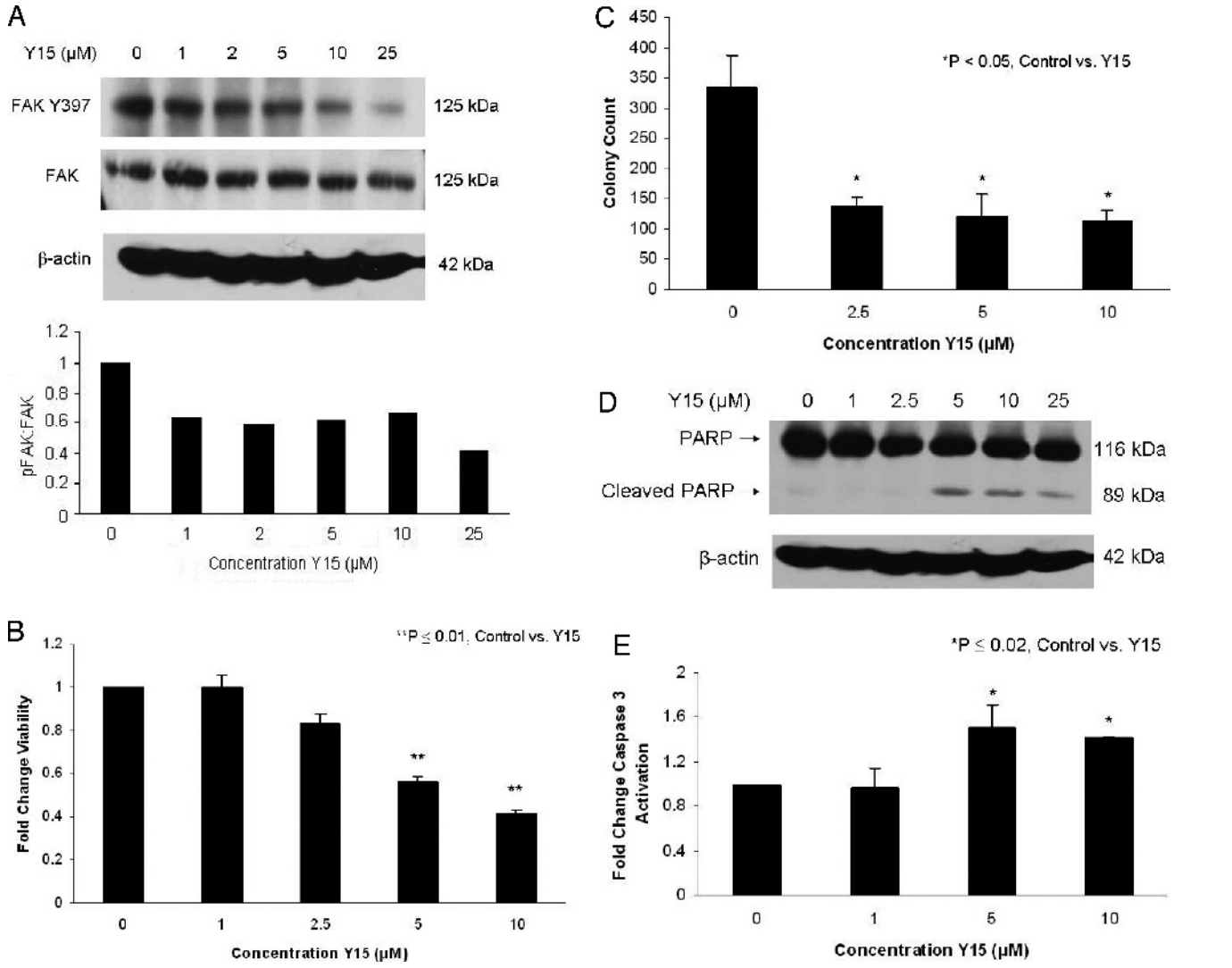

Figure 5. Y15 inhibition of FAK phosphorylation in HuH6 human hepatoblastoma cells. In anticipation of advancing to *in vivo* experiments, with the knowledge that PF was not formulated for animals, we began investigations with another small molecule FAK inhibitor, Y15. (A) HuH6 cells were treated for 48 hours with increasing concentrations of Y15 and cell lysates were obtained. Immunoblot analysis was used to examine FAK Y397 phosphorylation and total FAK in the lysates. Densitometry was performed, and FAK phosphorylation was reported as a ratio between the density of the Y397 phospho-FAK band to the density of the total FAK band. Increasing concentrations of Y15 resulted in decreased FAK phosphorylation. (B) AlamarBlue assay was used to measure cell viability. HuH6 hepatoblastoma cells were treated with Y15 at increasing concentrations for 48 hours. Cellular viability was decreased with treatment of 5 μM concentration. (C) Attachment-independent growth in soft agar was employed to further characterize tumor invasiveness. HuH6 cells were treated with increasing concentrations of Y15, grown in soft agar for 12 days, and colonies were quantified. Colony count was significantly decreased with Y15 treatment compared to untreated cells. (D) Since Y15 resulted in decreased cell survival, we examined the effects of Y15 on apoptosis in the HuH6 cells. HuH6 cells were treated with Y15 at increasing concentrations for 48 hours and lysates were examined with immunoblot analysis for PARP cleavage products. There was an increase in cleaved PARP beginning at the 5 μM concentration. (E) To further document apoptosis, HuH6 cells were treated for 48 hours with increasing concentrations of Y15. Apoptosis was measured with a caspase activation kit. Caspase-3 was significantly activated after Y15 treatment, corroborating the PARP cleavage data and indicating that Y15 treatment resulted in HuH6 cell apoptosis.

immunohistochemistry and that this overexpression of TLR4 was absent in eight of eight tumor specimens following chemotherapy. They also showed that the TLR4 agonist, lipopolysaccharide, inhibited motility and invasion of hepatoblastoma cells *in vitro* [20]. In 2007, Leaphart and colleagues reported that TLR4 coimmunoprecipitates with FAK and leads to FAK phosphorylation in intestinal endothelial cells [21]. Therefore, there may be potential for FAK to interact with TLR4 in hepatoblastoma. Previous studies have also demonstrated that PI3K and protein kinase B (AKT) played a role in hepatoblastoma cell survival [22,23]. Hartmann and colleagues found that 79% of human hepatoblastoma tumor specimens examined had strong expression of phospho-AKT [22]. In addition, inhibition of the PI3K pathway *in vitro* resulted in decreased proliferation of hepatoblastoma tumor cells and cellular apoptosis [22]. Recently, Wagner et al. found that inhibition of the AKT/mammalian target of rapamycin pathways with mammalian target of rapamycin inhibitors resulted in a significant decrease in tumor volume in a murine xenograft model of hepatoblastoma [23]. FAK has been shown to interact with the PI3K/AKT axis to

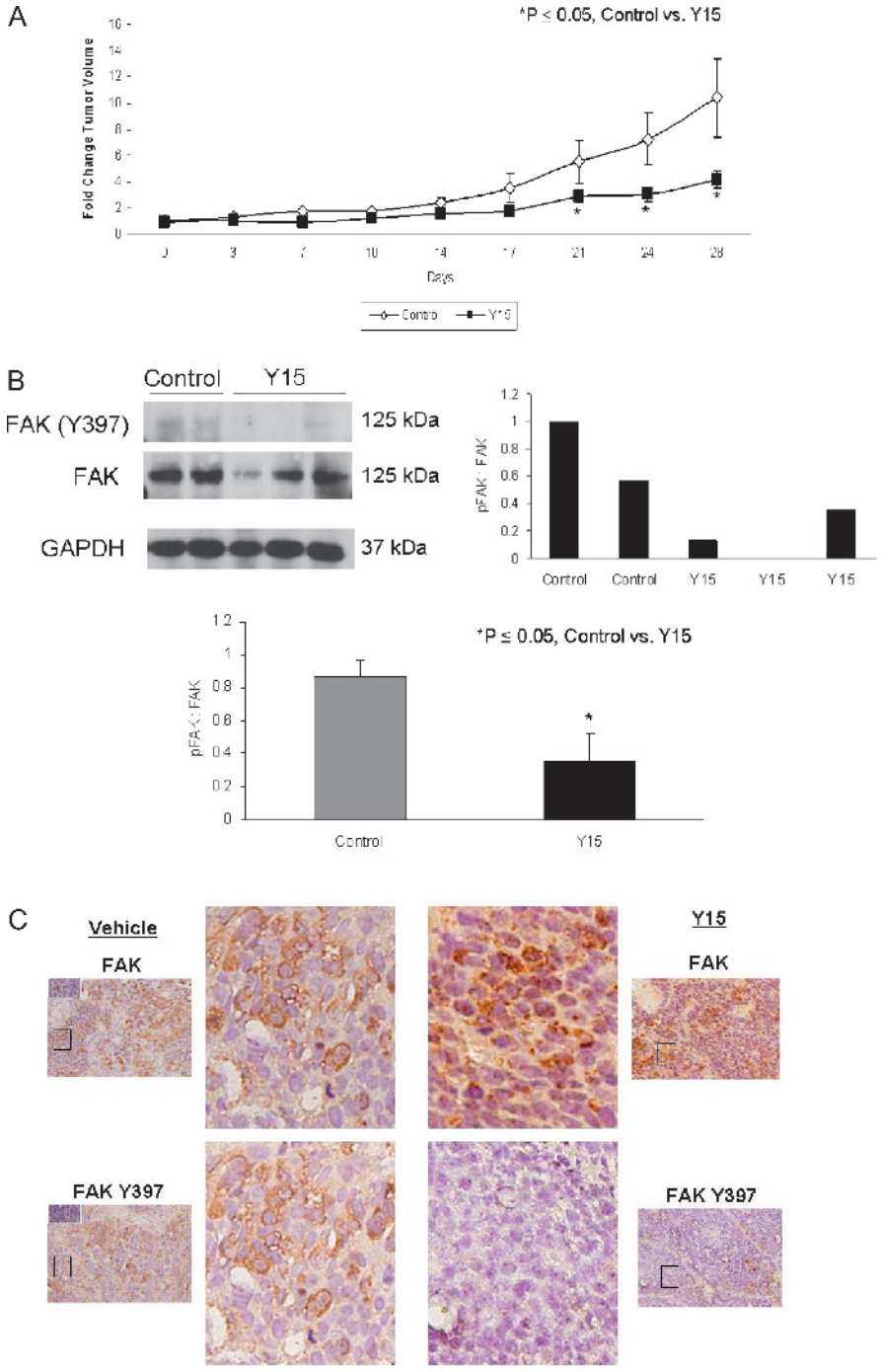

Figure 6. Treatment with Y15 inhibited growth of human hepatoblastoma xenografts. The investigations were advanced to a nude mouse xenograft model of hepatoblastoma. HuH6 cells were injected subcutaneously into the right flank. At the time of injection, animals were randomized to receive twice daily intraperitoneal injections of vehicle ($N = 9$, sterile normal saline, control, 100 μl) or Y15 ($N = 10$, 30 mg/kg/day, 100 μl). Animals were killed after 28 days treatment and their tumors harvested for study. (A) Tumor volumes were measured twice weekly with calipers and reported as fold change in tumor volume. In the animals receiving Y15 treatment, there was a significant decrease in the tumor volumes when compared to control-treated animals. (B) Tumors were homogenized and proteins were separated on SDS–polyacrylamide gel electrophoresis gels; immunoblot analysis for Y397 and total FAK were performed, with a representative immunoblot shown. There was a decrease in FAK phosphorylation (Y397) in the animals that received Y15 treatment (top left blot) that was further demonstrated by densitometry (top right graph). Immunoblots from a number of specimens were analyzed with densitometry. Phosphorylated FAK was expressed as a ratio to total FAK for each blot and normalized to the GAPDH for that blot, allowing for a comparison to be made between the saline-treated and the Y15-treated tumors. There was a significant decrease in the FAK phosphorylation (Y397) in the tumors from the animals treated with Y15 (bottom panel). (C) Representative photomicrographs at 20× of immunohistochemical staining of the formalin-fixed, paraffin-embedded HuH6 xenograft samples. The larger images correspond to the black boxes in photomicrographs. Immunohistochemical staining showed findings similar to immunoblot analysis; the tumors from the animals treated with Y15 had decreased FAK Y397 phosphorylation compared to the vehicle-treated tumors (bottom row). Negative controls were performed with each run (white inserts in left panels).

interrupt apoptotic pathways and increase tumor cell migration in breast and colorectal cancer, respectively [24,25]. The proven importance of PI3K/AKT in hepatoblastoma and the known cross talk between this pathway and FAK again lend credence to the hypothesis that FAK would be present and important to hepatoblastoma and support the need to begin to describe its role in this tumor.

In the current study, we found FAK expression in 23 of the 28 tumor specimens that were examined with immunohistochemistry. In addition, FAK was phosphorylated in the majority of these 28 hepatoblastoma specimens. A stain score was calculated for these specimens and the median stain score for FAK was 33.7. Although our numbers were too small to be used to determine prognostic significance and that was not the goal of the current investigation, on the basis of a previous study in neuroblastoma using the same stain scoring system [6], the stain scores for hepatoblastoma appear relevant. In the neuroblastoma study, the median stain score for FAK was 25, and FAK staining was noted to correlate with worse disease [6], with stain scores that were well below those noted in the current study. We also obtained the human hepatoblastoma cell line, HuH6, and confirmed that FAK was present and was phosphorylated at the Y397 site. After reviewing the literature, we determined that the characterization of FAK in hepatoblastoma has not previously been described.

Previously, researchers have proven that siRNA led to muted FAK expression with decreased cellular viability, decreased migration, and increased sensitivity to chemotherapy in lung, pancreatic, and other cancer cell lines [7,15,26,27]. For example, Han and others demonstrated a significant decrease in lung cancer cell soft agar colony formation following FAK abrogation with siRNA [7]. Walsh found that siRNA-induced FAK inhibition had a significant effect upon cellular adhesion to collagen in the human colon cancer cell line, SW620 [27]. In the current study, we showed through immunoblot analysis that FAK expression could be abrogated with RNAi in hepatoblastoma cells. In addition, this focused silencing of FAK resulted in decreased cellular viability in the HuH6 hepatoblastoma cells. RNAi techniques to inhibit FAK were employed to minimize potential off-target effects that could prove a potential critique of small molecule inhibition. These data were the first step to elucidating the effects of decreasing FAK in hepatoblastoma, prompting our investigations with small molecule FAK inhibitors.

Several small molecules have been isolated, which have been shown to inhibit the activity of FAK, including the compound PF and a similar compound PF-562,271. PF interacts with FAK in the adenosine triphosphate (ATP) binding pocket and blocks the catalytic activity of FAK [17]. The other compound, PF-562,271, is less selective, in that it also inhibits PyK2 [28], leading us to choose PF for our investigations in an attempt to limit potential off-target effects. In previous experiments, PF was shown to decrease adhesion and migration of human epithelial carcinoma cells [17] and small cell lung cancer cells [29] and to enhance chemotherapy-induced cytotoxicity and apoptosis in multiple human pancreatic cell lines [26]. Wendt et al. proved that inhibiting FAK with PF decreased invasion and metastatic potential in human breast cancer cells through blocking the FAK activation of transforming growth factor β [24]. Similar to previous descriptions, PF effectively inhibited FAK phosphorylation in the HuH6 cell line, resulting in decreased cellular viability and increased cellular apoptosis. In addition, other harbingers of increased tumorigenicity such as invasion, migration, and attachment-independent growth were inhibited with PF-induced FAK inhibition. The important point to note from this study was that invasion and migration were inhibited with concentrations of PF that were below those needed for a significant loss of viability.

PF is suitable for *in vitro* studies only [17]. Therefore, we chose another FAK inhibitor, Y15, which has been used for multiple *in vivo* studies [10–12]. Y15 is one of only a few small molecule FAK inhibitors that may be used in animal studies. Y15 has been shown previously to both directly inhibit autophosphorylation of FAK at the Y397 site and decrease total FAK expression [11,12]. Golubovskaya and others showed that Y15 treatment resulted in dose-dependent cellular detachment and decreased cellular viability in human breast cancer cells [10]. In addition, Y15 inhibition of FAK expression in neuroblastoma led to decreased cellular viability and attachment and increased apoptosis [12]. With evidence that Y15 caused decreased cell survival in other cancers and since it could be used *in vivo*, we chose to test its effects on human hepatoblastoma cells. Y15 treatment of these cells did result in diminished FAK phosphorylation. Further, treatment with Y15 resulted in decreased cellular viability, invasion, migration, and attachment-independent colony formation. Similar to PF, Y15 treatment also resulted in cellular apoptosis. Finally, as seen with the PF data, the decrease in migration and invasion seen in the cells occurred at a concentration of Y15 below that required for decreased viability. Certainly, the effects upon cellular viability from the small molecule inhibitors could be an off-target effect upon another cell survival signaling pathway other than FAK. However, RNAi inhibition of FAK resulted in similar findings to those of the small molecules, reducing the possibility of off-target effects.

Because of the effects of FAK inhibition *in vitro* with both RNAi and small molecule inhibitors, we advanced our investigations into a xenograft animal model of hepatoblastoma. Previous studies have shown that HuH6 cells will reliably form tumor xenografts in a murine model [24], and this was also true in our study. Further, we found that animals treated with Y15 had a significant decrease in their tumor volumes compared to animals treated with vehicle alone. In addition, there was a decrease in the target (FAK Y397) in the treated tumor xenografts by immunohistochemistry and a significant decrease in the pFAK/FAK ratio as detected by immunoblot analysis.

In conclusion, we believe that FAK plays an important role in the tumorigenicity of hepatoblastoma. Other investigators have been evaluating the efficacy of other kinase inhibitors in hepatoblastoma. Recently, the Aurora kinase inhibitor, VX-680, was shown *in vitro* to inhibit proliferation of HuH6 cells [30], indicating interest in the use of kinase inhibitors for this tumor. We believe that we have shown that FAK inhibition warrants further investigation as a potential therapeutic target in the treatment of hepatoblastoma.

Acknowledgments

The authors thank Thomas Pietschmann for his kind gift of the HuH6 human hepatoblastoma cell line and Elena Kurenova for the $MEF^{FAK+/+}$ and $MEF^{FAK-/-}$ cell lines.

References

[1] Stocker JT (1994). Hepatoblastoma. *Semin Diagn Pathol* **11**, 136–143.
[2] Davies JQ, de la Hall PM, Kaschula RO, Sinclair-Smith CC, Hartley P, Rode H, and Millar AJ (2004). Hepatoblastoma—evolution of management and outcome and significance of histology of the resected tumor. A 31-year experience with 40 cases. *J Pediatr Surg* **39**, 1321–1327.
[3] Xing A, Chen HC, Nowlen JK, Taylor SJ, Shalloway D, and Guan JL (1994). Direct interaction of v-Src with the focal adhesion kinase mediated by the Src SH2 domain. *Mol Biol Cell* **5**, 14–21.
[4] Chen HC and Guan JL (1994). Association of focal adhesion kinase with its potential substrate phosphatidylinositol 3-kinase. *Proc Natl Acad Sci USA* **91**, 10148–10152.

[5] Cance WG, Harris JE, Iacocca MV, Roche E, Yang X, Chang J, Simkins S, and Xu L (2000). Immunohistochemical analyses of focal adhesion kinase expression in benign and malignant human breast and colon tissues: correlation with preinvasive and invasive phenotypes. *Clin Cancer Res* **6**, 2417–2423.

[6] Beierle EA, Massoll NA, Hartwich J, Kurenova EV, Golubovskaya VM, Cance WG, McGrady P, and London WB (2008). Focal adhesion kinase expression in human neuroblastoma: immunohistochemical and real-time PCR analyses. *Clin Cancer Res* **14**, 3299–3305.

[7] Han EK, McGonigal T, Wang J, Giranda VL, and Luo Y (2004). Functional analysis of focal adhesion kinase (FAK) reduction by small inhibitory RNAs. *Anticancer Res* **24**, 3899–3905.

[8] Xu L, Yang X, Bradham C, Brenner D, Baldwin AJ, Craven R, and Cance W (2000). The focal adhesion kinase suppresses transformation-associated, anchorage-independent apoptosis in human breast cancer cells. Involvement of death receptor-related signaling pathways. *J Biol Chem* **275**, 30597–30604.

[9] Beierle E, Ma X, Trujillo A, Kurenova E, Cance W, and Golubovskaya V (2010). Inhibition of focal adhesion kinase and src increases detachment and apoptosis in human neuroblastoma cell lines. *Mol Carcinog* **49**, 224–234.

[10] Golubovskaya VM, Nyberg C, Zheng M, Kweh F, Magis A, Ostrov D, and Cance WG (2008). A small molecule inhibitor, 1,2,4,5-benzenetetraamine tetrahydrochloride, targeting the Y397 site of focal adhesion kinase decreases tumor growth. *J Med Chem* **51**, 7405–7416.

[11] Hochwald SN, Nyberg C, Zheng M, Zheng D, Wood C, Massoll NA, Magis A, Ostrov D, Cance WG, and Golubovskaya VM (2009). A novel small molecule inhibitor of FAK decreases growth of human pancreatic cancer. *Cell Cycle* **8**, 2435–2443.

[12] Beierle EA, Ma X, Stewart J, Nyberg C, Trujillo A, Cance WG, and Golubovskaya VM (2010). Inhibition of focal adhesion kinase decreases tumor growth in human neuroblastoma. *Cell Cycle* **9**, 1005–1015.

[13] Chen JS, Huang XH, Wang Q, Chen XL, Fu XH, Tan HX, Zhang LJ, Li W, and Bi J (2010). FAK is involved in invasion and metastasis of hepatocellular carcinoma. *Clin Exp Metastasis* **27**, 71–82.

[14] Haid S, Windisch MP, Bartenschlager R, and Pietschmann T (2010). Mouse-specific residues of claudin-1 limit hepatitis C virus genotype 2a infection in a human hepatocyte cell line. *J Virol* **84**, 964–975.

[15] Beierle EA, Trujillo A, Nagaram A, Kurenova EV, Finch R, Ma X, Vella J, Cance WG, and Golubovskaya VM (2007). N-MYC regulates focal adhesion kinase expression in human neuroblastoma. *J Biol Chem* **282**, 12503–12516.

[16] Golubovskaya VM and Cance WG (2007). Focal adhesion kinase and p53 signaling in cancer cells. *Int Rev Cytol* **263**, 103–153.

[17] Slack-Davis JK, Martin KH, Tilghman RW, Iwanicki M, Ung EJ, Autry C, Luzzio MJ, Cooper B, Kath JC, Roberts WG, et al. (2007). Cellular characterization of a novel focal adhesion kinase inhibitor. *J Biol Chem* **282**, 14845–14852.

[18] Fujii T, Koshikawa K, Nomoto S, Okochi O, Kaneko T, Inoue S, Yatabe Y, Takeda S, and Nakao A (2004). Focal adhesion kinase is overexpressed in hepatocellular carcinoma and can be served as an independent prognostic factor. *J Hepatol* **41**, 104–111.

[19] Yuan Z, Zheng Q, Fan J, Ai KX, Chen J, and Huang XY (2010). Expression and prognostic significance of focal adhesion kinase in hepatocellular carcinoma. *J Cancer Res Clin Oncol* **136**, 1489–1496.

[20] Hsiao CC, Kao YH, Huang SC, and Chuang JH (2012). TLR4 agonists inhibit migration and invasion of hepatoblastoma cells. *Pediatr Blood Cancer* **60**, 248–253

[21] Leaphart CL, Cavallo J, Gribar SC, Cetin S, Li J, Branca MF, Dubowski TD, Sodhi CP, and Hackam DJ (2007). A critical role for TLR4 in the pathogenesis of necrotizing enterocolitis by modulating intestinal injury and repair. *J Immunol* **179**, 4808–4820.

[22] Hartmann W, Küchler J, Koch A, Friedrichs N, Waha A, Endl E, Czerwitzki J, Metzger D, Steiner S, Wurst P, et al. (2008). Activation of phosphatidylinositol-3′-kinase/AKT signaling is essential in hepatoblastoma survival. *Clin Cancer Res* **15**, 4538–4545.

[23] Wagner F, Henningsen B, Lederer C, Eichenmüller M, Gödeke J, Müller-Höcker J, Schweinitz DV, and Kappler R (2012). Rapamycin blocks hepatoblastoma growth *in vitro* and *in vivo* implicating new treatment options in high-risk patients. *Eur J Cancer* **48**, 2442–2450.

[24] Schnater JM, Bruder E, Bertschin S, Woodtli T, de Theije C, Pietsch T, Aronson DC, von Schweinitz D, Lamers WH, and Köhler ES (2006). Subcutaneous and intrahepatic growth of human hepatoblastoma in immunodeficient mice. *J Hepatol* **45**, 377–386.

[25] Turecková J, Vojtechová M, Krausová M, Sloncová E, and Korínek V (2009). Focal adhesion kinase functions as an akt downstream target in migration of colorectal cancer cells. *Transl Oncol* **2**, 281–290.

[26] Huanwen W, Zhiyong L, Xiaohua S, Xinyu R, Kai W, and Tonghua L (2009). Intrinsic chemoresistance to gemcitabine is associated with constitutive and laminin-induced phosphorylation of FAK in pancreatic cancer cell lines. *Mol Cancer* **21**, 125.

[27] Walsh MF, Thamilselvan V, Groteluesche R, Farhana L, and Basson M (2003). Absence of adhesion triggers differential FAK and SAPKp38 signals in SW620 human colon cancer cells that may inhibit adhesiveness and lead to cell death. *Cell Physiol Biochem* **13**, 135–146.

[28] Roberts WG, Ung E, Whalen P, Cooper B, Hulford C, Autry C, Richter D, Emerson E, Lin J, Kath J, et al. (2008). Antitumor activity and pharmacology of a selective focal adhesion kinase inhibitor, PF-562,271. *Cancer Res* **68**, 1935–1944.

[29] Ocak S, Yamashita H, Udyavar AR, Miller AN, Gonzalez AL, Zou Y, Jiang A, Yi Y, Shyr Y, Estrada L, et al. (2010). DNA copy number aberrations in small-cell lung cancer reveal activation of the focal adhesion pathway. *Oncogene* **29**, 6331–6342.

[30] Dewerth A, Wonner T, Lieber J, Ellerkamp V, Warmann SW, Fuchs J, and Armeanu-Ebinger S (2012). *In vitro* evaluation of the Aurora kinase inhibitor VX-680 for hepatoblastoma. *Pediatr Surg Int* **28**, 579–589.

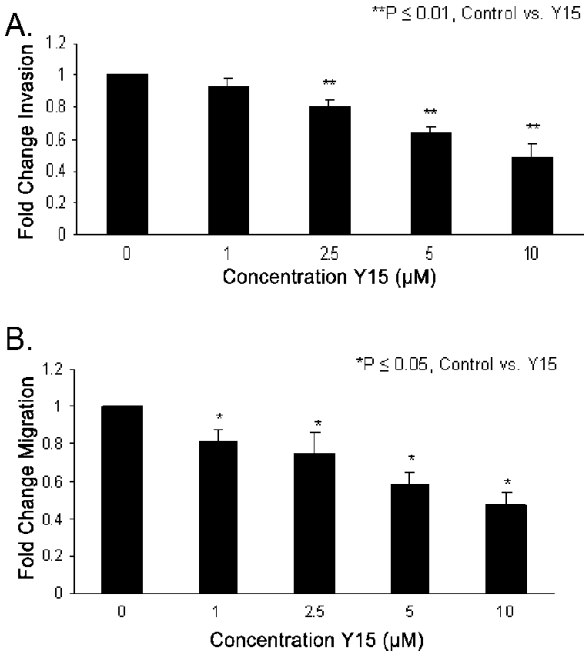

Figure W1. Y15 treatment of HuH6 cells led to decreased cellular invasion and migration. (A) HuH6 cells were treated with increasing concentrations of Y15 and allowed to invade through a Matrigel-coated micropore insert. Invasion was reported as fold change. Cellular invasion was significantly decreased with Y15 beginning at the 2.5 μM concentration. (B) HuH6 cells were treated with increasing concentrations of Y15 and allowed to migrate through a micropore insert. Migration was reported as fold change in number of cells migrating through the membrane. Cellular migration was significantly decreased with Y15 treatment at a concentration of 1 μM.